Highly Swollen Layered Nickel Oxide with a Trilayer Hydrate Structure

Xiaojing Yang,† Kazunori Takada, Masayuki Itose, Yasuo Ebina, Renzhi Ma, Katsutoshi Fukuda, and Takayoshi Sasaki*

International Center for Materials Nanoarchitectonics and Nanoscale Materials Center, National Institute for Materials Science, Namiki 1-1, Tsukuba, Ibaraki 305-0044, Japan

Received October 16, 2007. Revised Manuscript Received November 12, 2007

This paper reports the synthesis of alkali-free layered nickel oxides with a highly swollen hydrate structure, derived from $NaNiO_2$ through soft-chemical processes involving oxidation with bromine and subsequent acid treatment. Complete removal of interlayer Na^+ ions and subsequent hydration yielded a single phase of $H_xNiO_2 \cdot nH_2O$ ($x < 1$, $n \sim 1$) with an enlarged basal spacing of 9.6 Å. The materials had a monoclinic structure (*C*2/*m*); unit cell parameters for a typical composition of $H_{0.66}NiO_2 \cdot 0.9H_2O$ were $a = 4.8993(8)$ Å, $b = 2.8256(4)$ Å, $c = 9.7598(9)$ Å, and $\beta = 98.88(2)°$. Rietveld refinement revealed that the structure was composed of pseudohexagonal NiO_2 sheets accommodating partially occupied three layers of H_2O molecules and H_3O^+ ions in the galleries. The highly expanded layered structure is analogous to $Na_{0.3}NiO_2 \cdot 1.3H_2O$ and other layer oxides such as buserite-type manganese oxide and superconducting $Na_xCoO_2 \cdot yH_2O$ but differs in alkali-free composition. The 9.6 Å phase underwent partial dehydration to give a basal spacing of 7 Å upon exposure to atmosphere with a relative humidity of <30%.

Introduction

Layered nickel compounds including nickel oxyhydroxides have received increasing attention due not only to their electrochemical applications[1] but also to their novel properties arising from the two-dimensional triangular lattice structure within NiO_2 layers.[2,3] The α(II)- and γ(III)-type phases are two typical monolayer hydrate phases in the nickel system with low ($Z_{Ni} = 2$) and high oxidation states ($Z_{Ni} \geq 3$), respectively, where Z_{Ni} is the mean oxidation state of nickel. The α(II)-type phase has a turbostatic structure[4] accommodating hydrated anions; intercalation of bulky anions induces interlayer expansion from ~8 Å to, for instance, 13.2 Å in the case of the adipic solution. It was reported that the magnetic property is closely related to the basal spacing.[5] The γ(III)-type phase, formulated as $A_xH_yNiO_2(H_2O)_z$ (x, $y \leq 1$, A = alkali metal ions), is characterized by an interlayer distance of 7 Å.[6]

There are few studies on the hydration or swelling of layered nickel compounds with highly oxidized nickel, especially γ-type phase. Bode et al. reported that the hydrolysis of $NaNiO_2$ in various media leads to the formation of γ-type phase.[7] Nevertheless, it was difficult to prepare a pure γ-type phase, as it usually coexists with $Ni(OH)_2$ due to the dismutation of trivalent nickel[8] or with β(III)-NiOOH.[1h] Single γ-type phase was first successfully obtained by Bartl et al.[7b] via the repetitive oxidation of $NaNiO_2$ in solutions of NaOH and Br_2. Interestingly, Delmas et al. reported a coexisting minor phase with a large interlayer distance ~9.9 Å, which was formed during hydrolysis of $NaNiO_2$ in a buffered solution at pH ~9 or in a concentrated NaClO solution.[8a] This phase, however, has not been isolated.

* Corresponding author: Fax +81-29-854-9061; e-mail sasaki.takayoshi@nims.go.jp.

† Present address: College of Chemistry, P.O. Box S-46, Beijing Normal University, Beijing 100875, China.

(1) (a) Falk, S. U.; Salkind, A. J. Alkaline Storage Batteries; Wiley: New York, 1969. (b) Bacon, F. T. *J. Electrochem. Soc.* **1979**, *126*, 7C. (c) Molenda, J.; Stoklosa, A. *Solid State Ionics* **1990**, *38*, 1. (d) Liu, K. C.; Anderson, M. A. *J. Electrochem. Soc.* **1996**, *143*, 124. (e) Nam, K. W.; Kim, K. B. *J. Electrochem. Soc.* **2002**, *149*, A346. (f) Ohzuku, T.; Ueda, A.; Nagayama, M. *J. Electrochem. Soc.* **1993**, *140*, 1862. (g) Bardé, F.; Palacin, M. R.; Chabre, Y.; Isnard, O.; Tarascon, J.-M. *Chem. Mater.* **2004**, *16*, 3936. (h) Bardé, F.; Palacín, M. R.; Beaudoin, B.; Tarascon, J.-M. *Chem. Mater.* **2005**, *17*, 470.

(2) (a) Anderson, P. W. *Mater. Res. Bull.* **1973**, *8*, 153. (b) Borgers, P. F.; Enz, U. *Solid State Commun.* **1966**, *4*, 153. (c) Kemp, J. P.; Cox, P. A.; Hodby, J. W. *J. Phys.: Condens. Matter* **1990**, *2*, 6699. (d) Hirakawa, K.; Kadowaki, H.; Ubukoshi, K. *J. Phys. Soc. Jpn.* **1985**, *54*, 3526. (e) Matsumura, T.; Kanno, R.; Gover, R.; Kawamoto, Y.; Kamiyama, T.; Mitchell, B. J. *Solid State Ionics* **2002**, *152*, 303.

(3) (a) Bianchi, V.; Caurant, D.; Baffier, N.; Belhomme, C.; Chappel, E.; Chouteau, G.; Bach, S.; Pereira-Ramos, J. P.; Sulpice, A.; Wilmann, P. *Solid State Ionics* **2001**, *140*, 1. (b) Chappel, E.; Núñez-Regueiro, M. D.; Dupont, F.; Chouteau, G.; Darie, C.; Sulpice, A. *Eur. Phys. J. B* **2000**, *17*, 609. (c) Chappel, E.; Núñez-Regueiro, M. D.; Chouteau, G.; Isnard, O.; Darie, C. *Eur. Phys. J. B* **2000**, *17*, 615.

(4) (a) Figlarz, M.; Guenot, J.; Le Bihan, S. *C. R. Acad. Sci. Paris* **1970**, *C270*, 1079. (b) Genin, P.; Delahaye-Vidal, A.; Portemer, F.; Tekaia-Elhsissen, K.; Figlarz, M. *Eur. J. Solid State Inorg. Chem.* **1991**, *28*, 505. (c) Delahaye-Vidal, A.; Beaudoin, B.; Sac-Epée, N.; Tekaia-Elhsissen, K.; Audemer, A.; Figlarz, M. *Solid State Ionics* **1996**, *84*, 239. (d) Tekaia-Elhsissen, K.; Delahaye-Vidal, A.; Genin, P.; Figlarz, M.; Willmann, P. *J. Mater. Chem.* **1993**, *3*, 883.

(5) Taibi, M.; Ammar, S.; Jouini, N.; Fiévet, F.; Molinié, P.; Drillon, M. *J. Mater. Chem.* **2002**, *12*, 3238.

(6) Oliva, P.; Leonardi, J.; Laurent, J. F.; Delmas, C.; Braconnier, J. J.; Figlarz, M.; Fievet, F.; de Guibert, A. *J. Power Sources* **1982**, *8*, 229.

(7) (a) Bode, H.; Dehmelt, K.; Witte, J. *Z. Anorg. Allog. Chem* **1969**, *366*, 1. (b) Bartl, H.; Bode, H.; Sterr, G.; Witte, J. *Electrochim. Acta* **1971**, *16*, 615.

(8) (a) Delmas, C.; Braconnier, J. J.; Borthomieu, Y.; Figlarz, M. *Solid State Ionics* **1988**, *28*, 1132. (b) Delmas, C.; Borthomieu, Y.; Faure, C.; Delahaye, A.; Figlarz, M. *Solid State Ionics* **1989**, *32–33*, 104. (c) Delmas, C.; Fouassier, C.; Hagenmuller, P. *Mater. Res. Bull.* **1976**, *11*, 1483.

10.1021/cm702981a CCC: $40.75
Published on Web 12/22/2007

Park et al. reported the preparation of $Na_{0.3}NiO_2 \cdot 1.3H_2O$ phase with an interlayer distance of ~10 Å (in the deuterated water form), by oxidizing and hydrating Na_xNiO_2 in an $Na_2S_2O_8$ aqueous solution.[9] This phase has a bilayer hydrate structure similar to the layered compounds such as buserite-type manganese oxides[10,11] and a superconducting cobalt oxide of $Na_xCoO_2 \cdot yH_2O$.[12] Synthesis of highly oxidized and metastable NiO_2 phases was also attempted by total deintercalation of Li^+ ions from $LiNiO_2$. Extraction to $x < 0.3$ in Li_xNiO_2 was achieved via an electrochemical process[13,14] or a soft-chemical process.[1e,15] Starting from one of these phases, Arai et al.[16] recently reported that the insertion of alkali metal ions in their hydroxide solutions produced a series of γ-type phases containing Na^+ and K^+ forms.

Here, we present a highly swollen nickel oxide hydrate, $H_xNiO_2 \cdot nH_2O$ ($Z_{Ni} > 3$, $n \sim 1$), with a basal spacing of 9.6 Å. This structure was derived from α-$NaFeO_2$-type $NaNiO_2$. The hydrate was obtained in two steps: (1) chemically oxidizing $NaNiO_2$ with Br_2 leading to the single γ-type phase and (2) subsequently treating with an aqueous acid solution promoting extraction of Na^+ ions and enhanced swelling. The absence of alkali metal ions in the highly swollen interlayer space is one of the most noticeable structural features. The structure refinement and characterizations of this new oxide hydrate are reported herein.

Results and Discussion

Formation of Highly Swollen Layered Nickel Oxides. The highly swollen layered nickel oxide was prepared from $NaNiO_2$ by oxidative extraction of Na^+ ions and subsequent acid treatment. Figure 1 displays X-ray diffraction (XRD) patterns of $NaNiO_2$ and those oxidized by acetonitrile solutions of Br_2. Table 1 summarizes chemical analysis results of these samples.

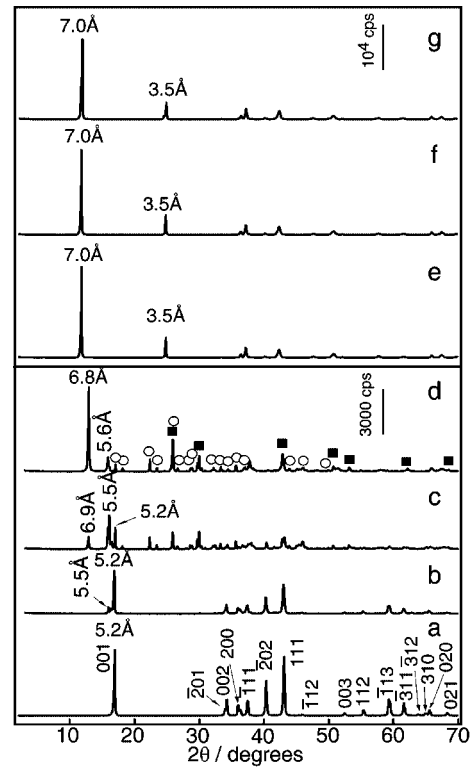

Figure 1. XRD patterns of the samples after (a) $NaNiO_2$ treated in Br_2/acetonitrile solutions at the Br/Ni molar ratios (b) 0, (c) 0.5, (d) 1, (e) 2, (f) 5, and (g) 10 followed by exposure to air overnight. Open circles and closed squares in (d) denote diffraction peaks attributable to NaBr (JCPDS 365-1456) and $NaBr \cdot 2H_2O$ (JCPDS 15-0010), respectively.

Table 1. Chemical Analysis Results of $NaNiO_2$, Samples Treated with Br_2/Acetonitrile Solution, and Then with H_2SO_4 Solution

sample	Ni/ wt %	Na/ wt %	H_2O/wt %	Z_{Ni}[a]	formula
as-prepared	49.6	19.2		2.97	$Na_{0.98}NiO_2$
Br/Ni = 0.5	37.0	13.9[b]	7.7	3.23	
Br/Ni = 1	35.8	13.3[b]	9.7	3.39	
Br/Ni = 2	51.6	6.8	9.2	3.63	$H_{0.02}Na_{0.33}NiO_2 \cdot 0.6H_2O$
Br/Ni = 5	53.4	7.0	9.2	3.63	$H_{0.03}Na_{0.33}NiO_2 \cdot 0.5H_2O$
Br/Ni = 10	53.7	6.8	9.2	3.61	$H_{0.07}Na_{0.32}NiO_2 \cdot 0.5H_2O$
H_2SO_4-treated	53.9	0	20.7	3.34	$H_{0.66}NiO_2 \cdot 0.9H_2O$

[a] Mean oxidation state of Ni. [b] NaBr and $NaBr \cdot 2H_2O$ were detected in the products by XRD.

The basal spacing of the as-prepared $NaNiO_2$ was 5.2 Å. It was confirmed by Rietveld refinement that the phase crystallizes in a *C*-base-centered monoclinic structure (see Supporting Information, Figure S1). The structure parameters obtained (Table S1) are consistent with previously reported data.[3b] The structure is composed of NiO_2 coplanar layers built up from edge-shared NiO_6 octahedra. Charge-balancing Na^+ ions are accommodated in an octahedral cavity produced by two neighboring NiO_2 layers.

The 5.2 Å phase was stable only in inert environments. A new basal peak at 5.5 Å appeared when brought into contact to ambient atmosphere, as seen in Figure 1b. The basal reflection at 5.2 Å further faded upon oxidation with Br_2/acetonitrile solution. These basal spacings coincide with those observed in the Na_xCoO_2 system: 5.2 and 5.5 Å for α-$NaCoO_2$ and β-Na_xCoO_2, respectively. α-$NaCoO_2$ has an

(9) (a) Park, S.; Kang, K.; Yoon, W.-S.; Moodenbaugh, A. R.; Lewis, L. H.; Vogt, T. *Solid State Commun.* **2006**, *139*, 60. (b) Park, S.; Lee, Y.; Elcombe, M.; Vogt, T. *Inorg. Chem.* **2006**, *45*, 3490.
(10) (a) Wadsley, A. D. *J. Am. Chem. Soc.* **1950**, *72*, 1781. (b) Giovanoli, R.; Stähli, E.; Feitknecht, W. *Helv. Chim. Acta* **1970**, *53*, 209; **1970**, *53*, 453. (c) Potter, R. M.; Rossman, G. R. *Am. Mineral.* **1979**, *64*, 1199.
(11) (a) Silvester, E.; Charlet, L.; Manceau, A. *J. Phys. Chem.* **1995**, *99*, 16662. (b) Feng, Q.; Kanoh, H.; Miyai, Y.; Ooi, K. *Chem. Mater.* **1995**, *7*, 1722. (c) Luo, J.; Zhang, Q.; Huang, A.; Giraldo, O.; Suib, S. L. *Inorg. Chem.* **1999**, *38*, 6106. (d) Chen, R. J.; Zavalij, P.; Whittingham, M. S. *Chem. Mater.* **1996**, *8*, 1275.
(12) (a) Takada, K.; Sakurai, H.; Takayama-Muromachi, E.; Izumi, F.; Dilanian, R. A.; Sasaki, T. *Nature (London)* **2003**, *422*, 53. (b) Takada, K.; Sakurai, H.; Takayama-Muromachi, E.; Izumi, F.; Dilanian, R. A.; Sasaki, T. *J. Solid State Chem.* **2004**, *177*, 372. (c) Takada, K.; Fukuda, K.; Osada, M.; Nakai, I.; Izumi, F.; Dilanian, R. A.; Kato, K.; Takata, M.; Sakurai, H.; Takayama-Muromachi, E.; Sasaki, T. *J. Mater. Chem.* **2004**, *14*, 1448. (d) Takada, K.; Sakurai, H.; Takayama-Muromachi, E.; Izumi, F.; Dilanian, R. A.; Sasaki, T. *Adv. Mater.* **2004**, *16*, 1901. (e) Takada, K.; Sakurai, H.; Takayama-Muromachi, E.; Izumi, F.; Dilanian, R. A.; Sasaki, T. *Physica C* **2004**, *412–14*, 14. (f) Sakurai, H.; Takada, K.; Izumi, F.; Dilanian, R. A.; Sasaki, T.; Takayama-Muromachi, E. *Physica C* **2004**, *412–14*, 182. (g) Takada, K.; Osada, M.; Izumi, F.; Sakurai, H.; Takayama-Muromachi, E.; Sasaki, T. *Chem. Mater.* **2005**, *17*, 2034.
(13) Li, W.; Reimers, J. N.; Dahn, J. R. *Solid State Ionics* **1993**, *67*, 123.
(14) (a) Croguennec, L.; Pouillerie, C.; Delmas, C. *J. Electrochem. Soc.* **2000**, *147*, 1314. (b) Croguennec, L.; Pouillerie, C.; Mansour, A. N.; Delmas, C. *J. Mater. Chem.* **2001**, *11*, 131.
(15) (a) Arai, H.; Sakurai, Y. *J. Power Sources* **1999**, *81–82*, 401. (b) Arai, H.; Tsuda, M.; Saito, K.; Hayashi, M.; Takei, K.; Sakurai, Y. *J. Solid State Chem.* **2002**, *163*, 340.
(16) Arai, H.; Tsuda, M.; Hayashi, M.; Ohtsuka, H.; Sakurai, Y. *Electrochim. Acta* **2005**, *50*, 1821.

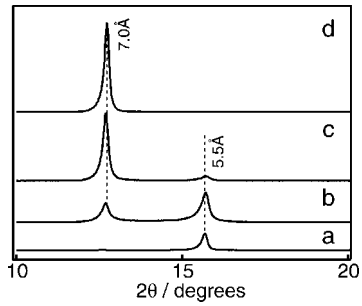

Figure 2. Hydration process of the as-oxidized sample (Br/Ni = 5) at RH = 10%. (a) As-oxidized. Exposing time for (b−d) is 1 min, 1 h, and 12 h, respectively. The data for (a) were recorded with special care to keep the sample from moisture, as described in the Experimental Section. Air with a controlled RH of 10% was used to monitor the phase evolution. Changes at higher RHs were too fast to follow.

O3 structure, in which Na^+ ions occupy octahedral sites in the galleries. Deintercalation of Na^+ ions promotes transformation of α-$NaCoO_2$ into β-Na_xCoO_2 with a P3 structure; CoO_2 layers glide, changing the octahedral coordination environment for Na^+ ions to a trigonal-prismatic one.[17] By taking into account that $NaNiO_2$ has a very similar crystal structure to α-$NaCoO_2$, the nearly identical basal spacing of the Ni oxide and Co oxide systems suggests that such transformation also took place in the former system during the Br_2 treatment. That is, Na^+ deintercalation transforms pseudo-O3-type $NaNiO_2$[18] into P3 Na_xNiO_2 accompanied by expansion of interlayer distance from 5.2 to 5.5 Å. Spontaneous oxidation of the pristine $NaNiO_2$ upon exposure to ambient atmosphere may be consistent with electrochemical data previously reported,[19] showing highly oxidative nature of the sample.

Further oxidation using a larger dose of Br_2 developed a reflection at $d = 7$ Å (Figure 1c). This is ascribed to the formation of the γ-phase,[6] in which H_2O molecules are accommodated in the galleries in addition to Na^+ ions. This hydration proceeded upon exposure of the as-oxidized sample to ambient atmosphere. In practice, XRD data indicated the formation of anhydrated phase with the interlayer distance of 5.5 Å just after the treatment with Br_2, which was immediately transformed into the 7 Å phase upon exposure to humid air (see Figure 2). A similar behavior, uptake of moisture, has been demonstrated in the γ-Na_xCoO_2 system, although it was much slower.[12b] The weakened attraction between the NiO_2 layers may be responsible for the insertion of H_2O molecules transforming as-oxidized Na_xNiO_2 to γ-phase. Oxidation with Br_2 reduced the negative charge density in the NiO_2 layers and the positive charge density in the interlayer space, hence weakening the electrostatic attraction between layers. This change makes the interlayer gallery easily prop open to insert H_2O molecules.

The larger dose of Br_2 tended to promote the transformation, producing single γ-phase when the molar ratio of Br/Ni was 2 and above (Figure 1e−g). However, treatment with large excess of Br_2 did not bring about any changes. Redox potential of Ni^{3+}/Ni^{4+} depends on the Na content. The Na deintercalation proceeds until it reaches the redox potential of Br^-/Br_2 and then is terminated. Therefore, further doses did not bring about a marked change in the diffraction pattern, Na content, or Z_{Ni} value (Table 1).

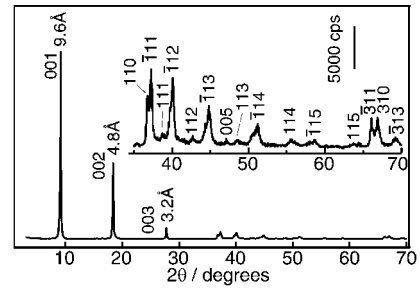

Figure 3. XRD pattern of the sample obtained by treating γ-type phase of $Na_{0.33}NiO_2 \cdot 0.5H_2O$ with 0.1 M H_2SO_4 for 24 h.

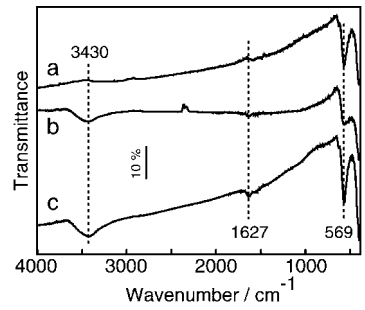

Figure 4. FT-IR spectra of samples (a) $NaNiO_2$, (b) γ-type phase of $Na_{0.33}NiO_2 \cdot 0.5H_2O$, and (c) 9.6 Å phase of $H_{0.66}NiO_2 \cdot 0.9H_2O$.

Soaking the γ-phase sample in a 0.1 M H_2SO_4 solution brought about new basal reflections at $d = 9.6$ Å, as shown in Figure 3. Such highly swollen phases have been found in layered oxides with a bilayer-hydrate structure[9–12] and hydrotalcite-like compounds.[20] H_2O molecules are coordinated to cationic species forming a double layer in the galleries in the former and to anionic species in the latter. Figure 4 shows Fourier transform infrared (FT-IR) spectra of the 9.6 Å phase and its precursors. The band at 569 cm^{-1} observed for $NaNiO_2$ is attributable to Ni−O lattice vibration.[4d] Transformation into γ-phase, i.e. insertion of H_2O molecules, produced two bands centered at around 3430 and 1627 cm^{-1}, which are assignable to stretching ν(O−H) and bending $\delta(H_2O)$ vibrations, respectively, of the H_2O molecules.[4c,d] These bands were also observed for the H_2SO_4-treated product (Figure 4c), whereas there was no band from SO_4^{2-} or CO_3^{2-}, which are possible intercalation species during acid treatment. Consequently, it is concluded that the 9.6 Å phase obtained is not a hydrotalcite related material but analogous to layered oxides with a bilayer-hydrate structure.

(17) Fouassier, C.; Matejka, G.; Reau, J.-M.; Hagenmuller, P. *J. Solid State Chem.* **1973**, *6*, 532.
(18) Braconnier, J. J.; Delmas, C.; Hagenmuller, P. *Mater. Res. Bull.* **1982**, *17*, 993.
(19) Because of slight distortion, $NaNiO_2$ adopts monoclinic lattice rather than rhombohedral structure. However, the structure is basically comparable to the so-called O3 structure in terms of the interlayer octahedral site.
(20) (a) Delmas, C.; Borthomieu, Y. *J. Solid State Chem.* **1993**, *104*, 345. (b) Han, K. S.; Guerlou-Demourgues, L.; Delmas, C. *Solid State Ionics* **1996**, *84*, 227. (c) Song, Q.; Tang, Z.; Guo, H.; Chan, S. L. I. *J. Power Sources* **2002**, *112*, 428. (d) Cerc Korošec, R.; Bukovec, P.; Pihlar, B.; Šurca Vuk, A.; Orel, B.; Dražič, G. *Solid State Ionics* **2003**, *165*, 191.

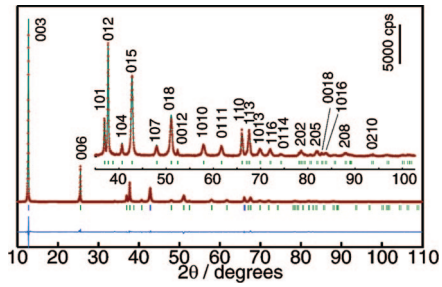

Figure 5. Rietveld refinement patterns for γ-phase of $Na_{0.33}NiO_2 \cdot 0.5H_2O$: observed (crosses), calculated (smooth line), and their difference (blue trace). The tick marks indicate the positions of allowed Bragg reflections.

The chemical formula for the 9.6 Å phase was determined to be $H_{0.66}NiO_2 \cdot 0.9H_2O$ on the basis of the chemical analysis results (Table 1). The Na content was substantially zero, while Z_{Ni} decreased to +3.34. This compositional change suggests a reaction scheme as follows: all Na^+ ions were exchanged for H^+ ions, and additional H^+ ions were inserted to reduce nickel ions during the H_2SO_4 treatment. Actually some bubbles evolved, implying that Ni^{4+} ions underwent reduction to Ni^{3+}, oxidizing H_2O to generate O_2 gas.

It should be noted that the treatment of the γ-phase with water instead of H_2SO_4 solution only produced two small XRD peaks attributable to the swelling to the interlayer separation of 10 Å while the γ-phase structure with $d = 7$ Å remained nearly unchanged as a main component (see Supporting Information, Figure S3). This minor 10 Å phase may be similar to the phase with Na^+ reported by Park et al.[9] This result indicates the importance of H_2SO_4 treatment to isolate the alkali-free phase with the largely expanded interlayer distance of 9.6 Å.

Crystal Structures. The Ni ions in nickel oxides have mixed valence between +3 and +4. Ni^{3+} ions bring about Jahn–Teller distortion, while Ni^{4+} ions do not. Therefore, during the soft chemical reactions, not only does the insertion of H_2O molecules change the interlayer structure but also the change in Z_{Ni} modifies the NiO_2 layers themselves. All the Ni ions are in a trivalent state in $NaNiO_2$, distorting the lattice to monoclinic, which was confirmed by XRD[21] and neutron diffraction studies.[3b]

Bartl et al.[7b] determined the structure for γ-phase of $NaNi_3O_6 \cdot 2H_2O$ to be *C*-centered monoclinic (*C*2/*m*; $a = 4.9$ Å, $b = 2.83$ Å, $c = 7.17$ Å, $\beta = 103.1°$), while Delmas et al.[8a] reported that γ-phase formed in the hydrolysis of $NaNiO_2$ (via disproportion reaction of Ni^{3+}) had a rhombohedral lattice (hexagonal parameters: $a = 2.82$ Å and $1/3c = 7.02$ Å). Our sample did not show significant monoclinic distortion and was very similar to the latter; all the reflections were indexable on the basis of the space group with rhombohedral symmetry ($R\bar{3}m$), as shown in Figure 5. When the structure was refined on the basis of structure models belonging to space groups *C*2/*m* as well as $R\bar{3}m$, *R* factors from *C*2/*m* symmetry were not significantly lower than those from $R\bar{3}m$ (Table 2). Accordingly, it can be concluded that the Br_2 treatment relaxed the Jahn–Teller distortion to adopt the rhombohedral lattice as a consequence of decrease in the amount of Ni^{3+} ions. Figure 6a illustrates the refined crystal structure, in which Na^+ ions and H_2O molecules are accommodated in a monolayer between NiO_2 host layers.

Table 2. Structure Parameters of γ-Phase $Na_{0.33}NiO_2 \cdot 0.5H_2O$

atom	Wyckoff index	occupancy	*x*	*y*	*z*	*U*/Å^2
Ni	3a	1	0	0	0	0.0134(8)
O	6c	1	0	0	0.6212(2)	0.014(1)
Na	18g	0.055	0.203(5)	0	1/2	0.026(8)
WO	9d	0.18	1/2	0	1/2	0.050(7)

[a] Space group: $R\bar{3}m$ (No. 166); $a = 2.8295(2)$ Å, $c = 20.9472(7)$ Å, $V = 145.23(2)$ Å^3; virtual species WO, whose atomic scattering factors were set equal to the sums of those of one O and 2 H atoms. $R_{wp} = 15.38\%$, $R_p = 10.22\%$, $R_B = 2.47\%$, $R_F = 2.39\%$, $R_R = 12.67\%$, $S = 1.63$.

The formation of the 9.6 Å phase was accompanied by the reduction of Ni^{4+} ions to Ni^{3+}, which distorts the lattice again: all reflections could be indexed based on *C*2/*m* (Figure 3). The structural change was analyzed through Rietveld refinement procedure. Since the interlayer species of H_2O molecules and H_3O^+ ions are highly disordered in the arrangement, their positions were examined by the maximum-entropy method (MEM) based pattern fitting.[12a,22] The MEM pattern gave clear peaks of electron density in the interlayer gallery (Figure 6b), which are arranged in trilayer. We took these peaks as the positions of H_2O molecules and H_3O^+ ions and refined the structure on the basis of this model. The final structure parameters and fitting result are shown in Table 3 and Figure 7, respectively. The sufficiently low *R* factors supported the structure model. The structure is composed of NiO_2 coplanar sheets with three layers of H_2O/H_3O^+ between them. In the trilayer structure, the central layer is occupied by W_xO1 while each of outer layers is both by W_xO2 and W_xO3.

The structure is analogous to the layer oxides of $Na_{0.3}NiO_2 \cdot 1.3H_2O$,[9] buserite-type manganese oxide,[10,11] and superconducting $Na_xCoO_2 \cdot yH_2O$,[12] in that they contain three discrete layers of guest species in the interlayer domain. However, those compounds accommodate alkali ions solvated by two layers of H_2O molecules, whereas three layers of H_2O/H_3O^+ pillar the galleries in the present hydrated nickel oxide. The distances between the interlayer H_2O molecules and H_3O^+ ions (W_xO species in Table 3) are 1.5–2.1 Å, which are apparently too short for these species. However, these sites are partially occupied. In fact, the refinement indicated that each of the sites of the W_xO species had a low occupancy factor, 0.30, 0.19, and 0.12. The partial occupancies suggest that H_2O molecules and H_3O^+ ions can be separated at a reasonable distance (>2.5 Å) in the real structure.

(21) Dyer, L. D.; Borie, B. S., Jr.; Smith, G. P *J. Am. Chem. Soc.* **1954**, *76*, 1499.

(22) (a) Izumi, F.; Ikeda, T. *Mater. Sci. Forum* **2000**, *321–324*, 198. (b) Takata, M.; Umeda, B.; Nishibori, E.; Sakata, M.; Saito, Y.; Ohno, M.; Shinohara, H. *Nature (London)* **1995**, *377*, 46. (c) Izumi, F.; Dilanian, R. A. In *Resent Research Developments in Physics*; Transworld Research Network: Trivandrum, 2003; Vol. 3, Part II, pp 699–726. (d) Izumi, F. http://homepage.mac.com/fujioizumi/index.html.

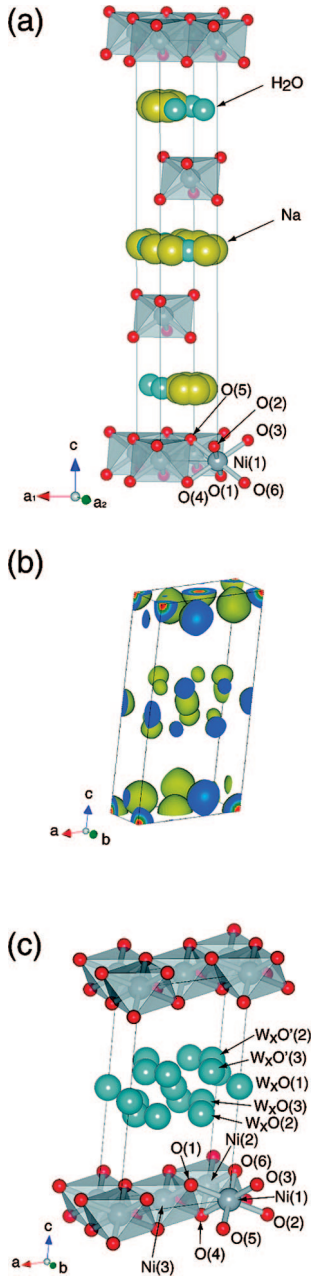

Figure 6. (a) Crystal structure for γ-type phase of $Na_{0.33}NiO_2 \cdot 0.5H_2O$. (b) Isosurfaces of electron densities for 9.6 Å phase of $H_{0.66}NiO_2 \cdot 0.9H_2O$ determined by MEM where the density level is 1.0 $Å^{-3}$, on the incisions (the spectrum form): red = maximum; blue = minimum. (c) Crystal structure for 9.6 Å phase of $H_{0.66}NiO_2 \cdot 0.9H_2O$. Selected interatomic distances (in Å) for (a): Ni−O 1.891(2); Ni−Ni 2.8295(2); and the shortest H_2O-O_{layer} 2.906(3). For (c): Ni(1)−O(1) and Ni(1)−O(2) 1.853(8); Ni(1)−O(3), Ni(1)−O(4), Ni(1)−O(5), and Ni(1)−O(6) 1.836(4); Ni(1)−Ni(2) 2.8256(4); Ni(1)−Ni(3) 2.8279(3); $H_xO(2)-O(1)$ 3.09(5).

In order to evaluate the degree of Jahn–Teller distortion, a distortion index σ_{JT} defined by the following formula[23] was calculated from the structure parameters refined above:

$$\sigma_{JT} = \sqrt{\frac{1}{6}\sum_{i=1}^{6}[(\mathrm{Ni-O})_i - \langle \mathrm{Ni-O}\rangle]^2} \qquad (1)$$

where $\langle$Ni−O$\rangle$ is the average bond length. The σ_{JT} for $NaNiO_2$, the γ-phase, and the 9.6 Å phase were 0.111, 0, and 0.008, respectively, which were in inverse order to Z_{Ni} or in the order of fraction of tetravalent nickel. The Jahn–Teller distortion is much smaller for the 9.6 Å phase than that in $NaNiO_2$, although not negligible.

Table 3. Structure Parameters of the Swollen Phase, $H_{0.66}NiO_2 \cdot 0.9H_2O$[a]

atom	Wyckoff index	occupancy	*x*	*y*	*z*	*U*/Å^2
Ni	2a	1	0	0	0	0.012(1)
O	4i	1	0.637(2)	0	0.9115(8)	0.035(2)
W_xO1[b]	2c	0.300 (2)	0	0	1/2	0.062(15)
W_xO2	4i	0.192(8)	0.330(6)	0	0.402(5)	$=U(W_xO1)$
W_xO3	4i	0.114[c]	0.229(10)	1/2	0.416(7)	$=U(W_xO1)$

[a] Space group: *C*2/*m* (No. 12); a = 4.8993(8) Å, b = 2.8256(4) Å, c = 9.7598(9) Å, β = 98.88(2)°, V = 133.49(3) Å^3. R_{wp} = 11.90%, R_p = 8.86%, R_B = 1.93%, R_F = 1.49%, R_R = 13.05%, S = 1.69. [b] Virtual species W_xO, for which the atomic scattering factors were set equal to the sums of those of 1 O and 2.72 H atoms. [c] Occupancy $g(W_xO3) = 0.46 - {}^1/_2 g(W_xO1) - g(W_xO2)$.

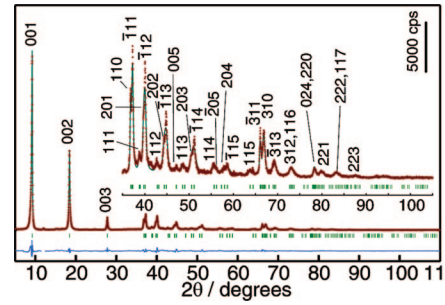

Figure 7. Rietveld refinement patterns for 9.6 Å phase of $H_{0.66}NiO_2 \cdot 0.92H_2O$: observed (crosses), calculated (smooth line), and their difference (blue trace). The tick marks indicate the positions of allowed Bragg reflections.

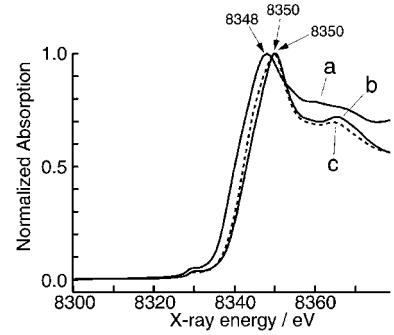

Figure 8. Normalized Ni K-edge XANES spectra for samples (a) $NaNiO_2$, (b) γ-type phase of $Na_{0.33}NiO_2 \cdot 0.5H_2O$, and (c) 9.6 Å phase of $H_{0.66}NiO_2 \cdot 0.9H_2O$.

The X-ray absorption near-edge structure (XANES) spectra (Figure 8) also supported the above conclusions on the chemical and structural features of the samples. The positions of the absorption edge reflecting Z_{Ni}[24,25] were in the order of $NaNiO_2$, the 9.6 Å phase, and γ-phase. The order is in good agreement with that of Z_{Ni} determined by chemical analysis (Table 1). The weak pre-edge peaks around 8330 eV are assigned to the 1s → 3d transition.[24] Although this transition is forbidden, hybridization of p and d states caused

(23) (a) Radaelli, P. G.; Iannone, G.; Marezio, M.; Hwang, H. Y.; Cheong, S.-W.; Jorgensen, J. D.; Argyriou, D. N. *Phys. Rev. B* **1997**, *56*, 8265. (b) Chi, E.-O.; Hong, K.-P.; Kwon, Y.-U.; Raju, N. P.; Greedan, J. E.; Lee, J.-S.; Hur, N. H. *Phys. Rev. B* **1999**, *60*, 12867.

(24) (a) Pandya, K. I.; Höffman, R. W.; McBreen, J.; O'Grady, W. E. *J. Electrochem. Soc.* **1990**, *137*, 383. (b) Pandya, K. I.; O'Grady, W. E.; Corrigan, D. A.; McBreen, J.; Hoffman, R. W. *J. Phys. Chem.* **1990**, *94*, 21.

(25) Bianconi, A. In *X-Ray Absorption*; Koningsberger, D. C., Prins, R., Eds.; Wiley: New York, 1988; p 573.

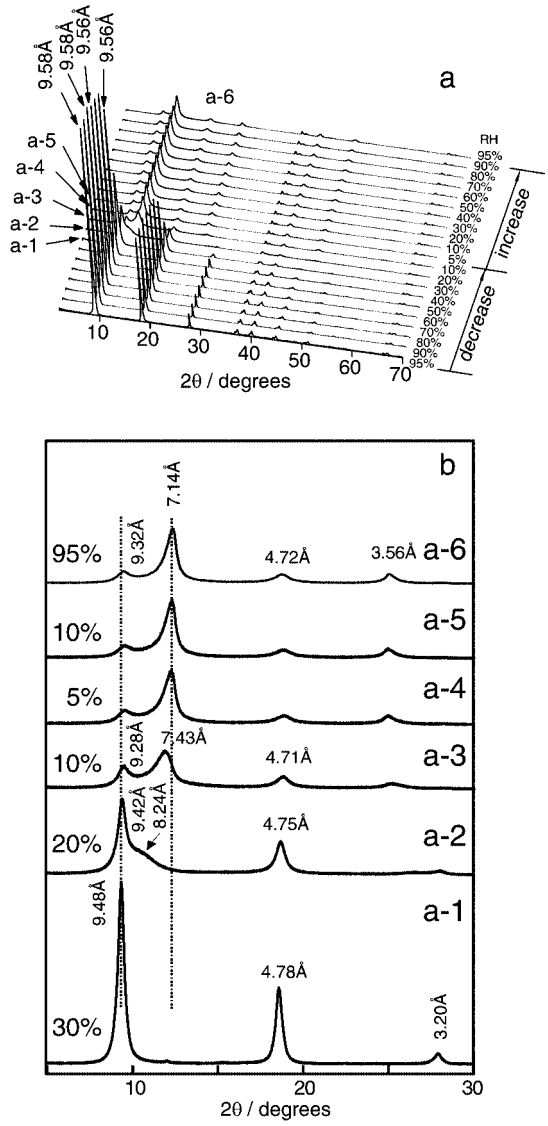

Figure 9. (a) 3D and (b) expanded XRD patterns of 9.6 Å phase of $H_{0.66}NiO_2 \cdot 0.9H_2O$ recorded at variable RHs.

by the asymmetry, or distortion in the coordination, partially allows the transition. Therefore, the intensity of the pre-edge peak strongly depends on the coordination symmetry of the Ni site.[25] The intensity was lower for the γ-phase and the 9.6 Å phase than for $NaNiO_2$, indicating that the NiO_6 octahedra in the former are less distorted.

Dehydration/Rehydration Behavior. The 9.6 Å phase is highly hydrated although it does not contain alkali metal ions. Generally interlayer alkali metal ions, particularly smaller ones such as Li^+ and Na^+, attract a larger number of H_2O molecules, resulting in a well-expanded interlayer spacing.[9–12] Therefore, it is of interest to clarify how this phase undergoes dehydration.

The 9.6 Å phase was dehydrated either by exposure to dry atmosphere or by heat treatment. As shown in Figure 9a, the 9.6 Å phase remained unchanged until the relative humidity (RH) decreased to 30%, except for a slight interlayer shrinkage to 9.5 Å (Figure 9a-1). A new reflection at $d = 8.2$ Å appeared (Figure 9a-2) when RH decreased to 20%, and it developed and shifted to $d = 7.1$ Å (Figure 9a-3,a-4), while the reflection at $d = 9.5$ Å decreased in intensity and shifted to 9.3 Å. The basal spacing of 7.1 Å is characteristic of a monolayer-hydrate structure. Similar transformation from a bilayer-hydrate structure to a monolayer-hydrate one under low RH conditions takes place in other systems such as superconducting layered cobalt oxides[12b,f] and buserite manganese oxides.[11d] The resultant monolayer-hydrate phases are rehydrated to the original bilayer-hydrate ones upon exposure to high-RH atmosphere. However, in the present case, the bilayer-hydrate phase was not restored from the 7 Å phase even when RH was increased to 95% (Figure 9a).

Conclusions

The highly swollen layered $H_xNiO_2 \cdot yH_2O$ ($x < 1$, $y \sim 1$) with the basal spacing of 9.6 Å was synthesized from $NaNiO_2$ through the soft-chemical route involving oxidative deintercalation of Na^+ ions using Br_2 and subsequent immersion in a H_2SO_4 solution. The first step transformed $NaNiO_2$ to γ-$Na_xNiO_2 \cdot nH_2O$ ($x \approx 0.33$), and the second step removed all residual Na^+ ions in the galleries and induced the high degree of hydration. This is the first highly swollen phase with trilayers of H_2O/H_3O^+ that does not have alkali metal ions as intercalation guests.

Experimental Section

Materials. Reagents used were of analytical grade and higher purity. Milli-Q-filtered ultrapure water (resistivity >18 MΩ cm) was used in the present study.

$NaNiO_2$ was prepared by solid-state reaction from Na_2O_2 and NiO. Na_2O_2 (3.65 g) and NiO (7.00 g) with a molar ratio of Na/Ni = 1.05 were mixed in an Ar-filled glovebox and placed in an Al_2O_3 boat. The mixture was heated at 700 °C for 70 h under an O_2 gas flow and then allowed to cool to room temperature. The black powder obtained had a composition of $Na_{0.98}NiO_2$ ($Z_{Ni} = 2.97$).

Oxidation Process. The powder sample of $NaNiO_2$ (1 g) was placed in the acetonitrile solution (100 cm^3) of Br_2 in various concentrations. After intermittently shaking for 3 days, the solid was filtered, washed with acetonitrile several times, and then air-dried.

Acid Treatment. The γ-phase sample (1 g) was shaken in a 0.1 M H_2SO_4 aqueous solution (100 cm^3) at room temperature for 24 h. After being filtered and then washed several times with water, the black solid powder was conditioned in a desiccator with RH = 93% in order to reach the constant water content.

Chemical Analysis. Contents of Na and Ni were determined by inductively coupled plasma atomic emission spectroscopy (ICP-AES) after the samples were dissolved in a 6 M HCl solution. The mean oxidation state of Ni, Z_{Ni}, was analyzed by iodometry[15,21] after dissolved in a aqueous solution of 6 M HCl and KI under nitrogen gas.

The water content was analyzed by an RC-412 type multiphase carbon, hydrogen, and moisture determinator (LECO Corp.). An amount of released water was determined by heating the sample at 500 °C for 180 s under nitrogen gas flow. Calibration was carried out using sodium tungsten oxide (99.5–100%, Kanto Chem. Co. Japan) as standard substance. For the samples without sodium, the water content was calculated from the total weight loss in the thermogravimetric measurement. According to Na and Ni contents and Z_{Ni} values analyzed by the methods above, the proton contents were determined on the assumption of the total charge balance.

Instrumentation. XRD data at various RHs were collected on a powder diffractometer (RINT Ultima+ type of Rigaku) equipped with a RH-controllable sample chamber. In other cases, a RINT 2200-HF+ Ultima+/pc type diffractometer was employed. XRD data for a very hygroscopic sample of $NaNiO_2$ were recorded after loading it in a specially designed holder with an Al window in an Ar-filled dry box.

FT-IR absorption spectra were acquired on a Digilab S-45 spectrometer by KBr method. XANES measurements were performed at the Photon Factory BL-12C in the Institute of Materials Structure Science, High Energy Accelerator Research Organization (KEK-PF), Japan. Ni K-edge XAFS spectra calculated from the intensity ratio of transmitted X-ray to incident one were recorded in an energy range from 8300 to 8370 eV with an interval of 0.8 eV for the XANES region at room temperature.

Rietveld Refinement Details. Crystal structures for $NaNiO_2$ and the γ-phase of $Na_{0.33}NiO_2 \cdot 0.5H_2O$ were refined by Rietveld analysis procedure using the computer program RIETAN-2000.[22a] The structure refinement of the 9.6 Å phase was performed by the combination of Rietveld analysis,[22a,26] maximum-entropy method (MEM),[22b] and MEM-based pattern fitting (MPF).[22c] MEM was calculated by the program PRIMA.[22d]

The composition of $H_{0.66}NiO_2 \cdot 0.9H_2O$ (Table 1) strongly suggests that the galleries accommodate H_3O^+ ions as well as H_2O molecules as guests. A virtual chemical species, W_xO, was assigned to the guests in the Rietveld refinement. The atomic scattering factors of W_xO were set equal to the sums of those of 1 O and x H atoms (x is the H/O molar ratio in the interlayers). The content of W_xO was fixed to the analyzed composition. The sample was loaded to a sample holder by the side-packing method to suppress the preferred orientation. The possible preferred orientation was corrected by March−Dollase function with respect to the direction [0 0 1].

The guests of H_2O molecules and H_3O^+ ions were highly disordered, and thus, their positions were determined using the maximum-entropy method (MEM). The observed structure factors, F_O(Rietveld), were estimated by Rietveld analysis using several structure models with different guest arrangements, from which the electron density distribution in the unit cell was calculated by MEM. The unit cell was divided into $64 \times 64 \times 128$ pixels in the MEM calculations. The three-dimensional representation of the charge density distribution was visualized using VENUS software.[22d] Although different structure models were used in the analyses, peaks forming the trilayer were consistently observed in the electron density map, which were assigned as three sites for W_xO.

Acknowledgment. This work was supported by Japan Science and Technology Agency (JST).

Supporting Information Available: Rietveld refinement pattern, structure parameters, and crystal structure for $NaNiO_2$ and the XRD data for a sample obtained after treating the γ-phase, $Na_{0.33}NiO_2 \cdot 0.5H_2O$, with pure water. This material is available free of charge via the Internet at http://pubs.acs.org.

CM702981A

(26) Rietveld, H. M. *J. Appl. Crystallogr.* **1969**, *2*, 63.